SURFACE AREA EFFECTS ON PARTICULATE DRYING IN A ROTARY DRYER

Mohseni M.* and Peters B.
*Author for correspondence
University of Luxembourg, Faculty of Science, Technology and Communication,
Campus Kirchberg, 6, rue Coudenhove-Kalergi,
Luxembourg, L-1359,
E-mail: mohammad.mohseni@uni.lu

ABSTRACT

The objective of this study is analysis of drying process of wet wood particulates in a rotary dryer including dynamics motion using eXtended Discrete Element Method (XDEM). In this model, the particles are resolved as discrete phase coupled via heat, mass and momentum transfer to the surrounding gas phase. The influence of particle size distribution on drying rate and heat loss is evaluated. Moreover, the effect of inlet gas temperature and velocity on the particle bed mean temperature and moisture content is investigated. At the end, the particle temperature distribution in different instances during drying is visually presented.

INTRODUCTION

Generally, the rotary dryers are a kind of convective heat transfer devices which provide remarkable advantages such as good energy efficiency, better particle mixing and more effective drying. The operation of the rotary dryers is complicated due to the simultaneous heat and mass transfer between the solid and gas phases in addition to transport of particles through the dryer. The basic mechanism of drying consists of providing heat to the particles from the hot gas and evaporating water from particles into the gas phase. The water evaporation largely happens during the close contact between solid and gas phases that occurs in the fall stage and drying efficiency is closely related to the time of contact between two phases [1]. Each particle is heated up on its way from the inlet to the outlet of the dryer and the temperature at any given point in the dryer is constant, but the temperature varies along the length of the dryer [2]. During drying process the particle temperature remains at saturated temperature of water so that at atmospheric pressure it is around 100 °C. Due to the gas-solid flow characteristics, the rotary dryers are suitable for dealing with homogeneous and heterogeneous materials as well as sticky ones. Recently, rotary dryers have been employed to dry solid waste from processing of olives, woody biomass chips, carton packaging waste, alfalfa, as well as sewage sludge produced by wastewater treatment plants, which can be used as fertilizer [3].

NOMENCLATURE

C_p	[J/kg K]	Specific heat capacity at constant pressure
d_p	[m]	Particle diameter
D	[m^2/s]	Diffusion coefficient
h	[J/kg]	Enthalpy
K	[m^2]	Permeability
L_v	[J/kg]	latent heat of evaporation
m	[kg]	Mass
p	[Pa]	Pressure
Pr	[-]	Prandtl number
r	[m]	Radius; radial coordinate
Re	[-]	Reynolds number
t	[s]	Time
T	[K]	Temperature
V_g	[m/s]	Gas phase velocity

Special characters

δ	[-]	Differential operator
Δ	[-]	Difference
α	[W/m^2K]	Heat transfer coefficient
β	[m/s]	Mass transfer coefficient
λ	[W/mK]	Thermal conductivity
μ	[kg/ms]	dynamic viscosity
ν	[m^2/s]	Kinematic viscosity
ρ	[kg/m^3]	Density
τ	[-]	Tortuosity
σ	[W/m^2K^4]	Stefan-Boltzmann constant
ε_p	[-]	Particle porosity

Subscripts

l	liquid
g	gas
i	specie i
p	particle
s	solid
R	radius
0	initial value

The particulate drying with superheated steam as medium is an alternative to air which has some advantages such as increased efficiency, improved safety due to the reduced risk for fires and explosions, no odorous or particulate emissions, a combination of drying with material sterilization and pasteurization, and faster drying rates. [4, 5]

The conversion of the woody particles to energy could be done in two different ways via burning directly or gasifying to produce flammable gas which can be used for energy or converted into liquid fuel [6]. Based on Abbasfard et al. [7], the drying process takes place only in falling-rate period which means that the drying occurs below the critical moisture content and there is no constant-rate period which will be discussed and proved subsequently.

Commonly, the characteristics of particles and dimensions of dryer influence the drying time. According to Fernandes et al. [8] which analyses the hydrodynamic and drying aspects of a rotary dryer used in a fertilizer industry; when the drum rotates, the particles are conveyed around the wall perimeter because of centrifugal force for a certain distance and then fallen through the hot stream while drying occurs which is considered in this work. Also in Renaud et al. [9], numerous experiments are performed in a pilot-scale rotary dryer to show the significant influence of the solid moisture content and drying gas temperature on drying time. In addition, Ademiluyi ([3,10]) has studied the effects of drying parameters such as inlet air temperature, inlet air velocity, drum drive speed, feed rate, relative humidity of air, and feed drive speed on the specific heat transfer coefficient and heat load during drying of fermented ground cassava in a rotary dryer experimentally. It is shown that inlet air temperature, inlet air velocity, and feed rate have the most substantial effects on the specific heat transfer coefficient and the heat load in the material.

Based on the work by Johnson [11], the importance of particle size distribution on the disintegration of wet distiller spent grain compacts during drying in superheated steam is analysed. The results show that a decrease in particle size of the compact results in a decrease in the expansion of the compact during the warm-up period of superheated steam drying. Moreover, the paper by Stroem [5] evaluates the drying behaviour of Brewer's spent grain in a pilot-scale rotary superheated steam dryer. The evaluation is based on product moisture content, measurements of sticking and energy consumption. The results of an experimental design for three system parameters (steam temperature, steam velocity and feed rate) are presented so that the critical parameters with the most significant effect on the moisture content are feed rate and inlet steam temperature.

Furthermore, Castano [12] presents the modelling of a co-current rotary dryer designed as a benchmark for experimental purposes. This model system uses fine sand as the product to be dried because it is easily reusable. The input variables considered for this model are the feed flow of wet solid and the combustible fuel flow used to dry the product while considering the inlet flow of dry air to be constant. The main outputs of the model are the residual moisture of the dried product and the temperature of the exhaust air at the output of the drum. It is shown that the evaporation rate depends on the gas temperature, gas flow speed, grain moisture content and grain size. The mathematical modelling are developed in many studies such as Abbasfard et al. [7], Xu et al. [6] and Iguaz et al. [13] to simulate rotary dryer processes. They conclude that the most important parameters of rotary dryers which affect the final product properties are the initial solid moisture content and the gas temperature.

The drying rate is categorized to two types entitled as constant-rate and falling-rate periods. At constant-rate period the moisture movement within the solid is rapid enough to maintain a saturated condition at the surface, and the rate of drying is controlled by the rate of heat transferred to the evaporating surface. The rate of mass transfer balances the rate of heat transfer and the temperature of the saturated surface remains constant. While the falling-rate period begins at the critical moisture content when the constant-rate period ends. When the falling moisture content is above the critical moisture content, the whole drying process will occur under constant-rate conditions. If, on the other hand, the initial moisture content is below the critical moisture content, the entire drying process will occur in the falling-rate period. In total, a dynamic equilibrium establishes the rate of heat transfer to the material and the rate of vapour removal from the surface which is written as [14]:

$$dX / dt = h_t A \Delta t / L_v \quad (1)$$

where dX/dt is drying rate, h_t is total heat transfer coefficient, A is area for heat transfer and evaporation, and L_v is latent heat of evaporation. Basically, there are three transport phenomena inside a dryer that happen simultaneously during drying as heat transfer between particle and gas, wet particle transportation and water vapour transportation from particle to gas. The heat and mass transfer during transportation of particles inside dryer highly depend on the surface area and the contact time between particles and gas phase [4].

The drying analysis of a packed bed of particles in an immobile cylinder is studied by Mahmoudi et al. [15] using XDEM. In this work the same approach is applied on a moving bed of wood particles via employing a rotary dryer to investigate motion of particles on drying. And the emphasis is on bed surface area effects by implementing different particle size distribution on drying parameters such as drying rate and time, particle bed mean temperature and moisture content. Moreover, the spherical woody particles are applied and it is assumed that particle dimensions are constant during drying process which means the shrinkage is neglected. Also the motion of particles inside the drum is modelled. That is, the particles move through the rotary cylinder via rolling and sliding on the wall and then fall at the bottom of the bed which leads to better contact with gas phase and better heat transfer.

NUMERICAL METHOD

Generally, two techniques are used for describing fluid flow: Lagrangian and Eulerian. In the Eulerian approach, the flow is considered as continuous while the Lagrangian approach tracks the properties of each particle as it traverses in the flow [16]. The Lagrangian approach is used in XDEM to trace each particle individually so that it is suitable for the systems including a packed bed of particles in conjunction with gas phase. The process of thermal conversion is described by a set of one-dimensional and transient differential conservation

equations of mass, momentum and energy transfer applied to the solid and gaseous phase. In order to determine drying process, the evaporation temperature predicted by XDEM explains a drying front propagating into the particle. Thus, the particle is divided into a still wet part from its centre to the front and a dry region between the front and the outer surface. The predictions include major properties such as temperature and species distribution inside the particle [17]. For illustrating gas velocity within particle pores, the conservation equation of mass is written as:

$$\varepsilon_p \frac{\delta \rho_g}{\delta t} + \frac{1}{r^n} \frac{\delta (r^n \rho_g V_g)}{\delta r} = S_{mass} \qquad (2)$$

where ε_p, ρ_g, V_g and S_{mass} are particle porosity, gas density, gas velocity and mass source, respectively. To distinguish between different domains the variable *r* is specified as an infinite plate (n = 0), an infinite cylinder (n = 1) and a sphere (n = 2) which is used in this work since spherical woody particles are investigated. In addition, the Darcy law [18] is applied to implement gas species transport through particle pores so as the conservation equation of linear momentum for compressible flows within porous media is written as:

$$\frac{\varepsilon_p \mu_g}{K} = \frac{\delta (\varepsilon_p P)}{\delta r} \qquad (3)$$

where K and μ_g are gas permeability and viscosity, respectively. Besides, the conservation equation energy of solid phase is considered as:

$$\frac{\delta (\rho_s c_{p,s} T)}{\delta t} = \frac{1}{r^n} \frac{\delta}{\delta r} (r^n \lambda_{eff} \frac{\delta T}{\delta t}) + \sum_{i=1}^{k} \dot{w} H_k \qquad (4)$$

where the LHS term represents the accumulation of enthalpy. The first RHS term describes the contribution of the convective flow to the accumulation of enthalpy. The last RHS term represents the enthalpy from drying rate of *i* species (*i=1...k*). Thermal equilibrium between the gas and solid phases is assumed in the conservation equation of energy [19] and the effective thermal conductivity λ_{eff} is calculated as [20]:

$$\lambda_{eff} = \varepsilon_p \lambda_g + \eta \lambda_{solid} + (1-\eta) \lambda_{char} + \lambda_{rad} \quad (5)$$

where the RHS terms represent the participation of conductive heat transfer in gas, solid, char and by radiation, respectively. The latter is defined as:

$$\lambda_{rad} = \frac{4 \varepsilon_p}{1-\varepsilon_p} \sigma T^3 \qquad (6)$$

where σ is Stefan-Boltzmann constant. In order to describe species transport within a porous particle, the conservation equation for transfer of each specie concentration (*i*) in time and space between solid and gas phases during drying are written as [21]:

$$\frac{\delta Y_{i,g}}{\delta t} + \frac{1}{r^n} \frac{\delta (r^n Y_{i,g} V_g)}{\delta r} = \frac{1}{r^n} \frac{\delta}{\delta r} (r^n D_{i,eff} \frac{\delta Y_{i,g}}{\delta t}) + \dot{w}_{i,g} \qquad (7)$$

where $Y_{i,g}$ and $\dot{w}_{i,g}$ are gas specie (*i*) concentration and it's drying rate as a source term. As a result of the averaging process and the influence of tortuosity τ on the diffusion, an effective diffusion coefficient is introduced as:

$$D_{i,eff} = D_i \frac{\varepsilon_p}{\tau} \qquad (8)$$

where ε_p is particle porosity and D_i is molecular diffusion coefficients of (*i*) specie [21]. It should be noticed that species transport between solid and gas phases like vapour transfer in drying leads to particle density decrease or particle size reduction as shrinkage that the latter in neglected in this work [22,23].

VALIDATION

In order to validate the XDEM approach, drying of a single particle is verified with the experiments by Looi et al. [24]. The experimental device includes a drying chamber and a single particle located inside it. The inside diameter and the length of the drying chamber are approximately 25 and 100 mm, respectively. The apparatus is designed such that the rate of mass loss and the internal temperature of the particle could be continuously and simultaneously measured when drying is carried out in a pressurized superheated steam environment. The steam inlet is located at the lower end of the chamber and the steam exit at the top end. Two different experiments are simulated by XDEM and compared. The particle is considered as a spherical wet coal of diameters as 10 and 12 mm for cases A and B, respectively. The experiments are performed at the pressure of 2.4 bar, and the superheated steam temperature at 170 °C, as well as the steam velocity at 2.7 m/s. The Figure 1 shows prediction of particle core temperature done by XDEM compared to the experiments so that the results show a good agreement.

In addition, the Figure 2 shows drying rate behaviour according to the moisture content at the test temperature of 161 °C and pressure of 2.3 bar. The *AB* part on the curve represents a warming-up period of the particle. The *BC* part on the curve represents the constant-rate period which the particle temperature is constant during this period since heat transfer into the surface is constant and the heat is consumed just for water evaporation. While the surface temperature is constant, the free water during constant-rate period evaporates. After

finishing free water, the temperature starts to rise. This point is shown as point *C*, where the constant-rate ends and the drying rate falls. This is termed the critical-moisture content. The curved portion *CD* is termed the falling-rate period and is typified by a continuously changing rate throughout the remainder of the drying cycle. [14]

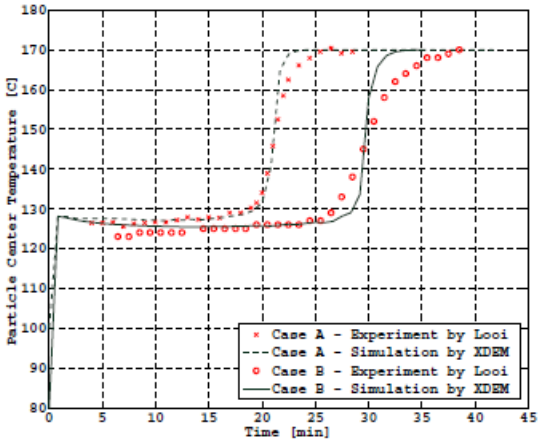

Figure 1 Particle size effect on single coal particle drying *Case A*: d_p=10[mm], P=2.4[bar], T_a=170[°C], v_g=2.7[m/s]; *Case B*: d_p=12[mm], P=2.3[bar], T_a=170[°C], v_g=2.7[m/s]

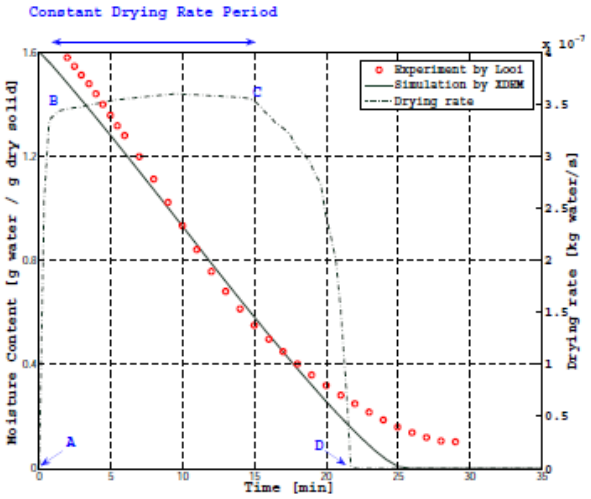

Figure 2 Experiment by Looi [24]: d_p=12[mm], P=2.3[bar], T_a=161[°C], v_g=2.7[m/s]

RESULTS AND DISCUSSIONS

As mentioned, the most important parameters that influence drying process in the rotary dryers are temperature and velocity of the inlet gas. In this section the effects of these parameters on the particle temperature and moisture content are assessed. Moreover, the effects of size distribution on the drying rate and the heat loss are discussed and finally the temperature distribution of particles in different instances during drying are visually exhibited.

Drum model

The case study is a rotary cylinder with geometry as length of 200 mm and diameter of 40 mm so that the drum axis is horizontal and the particles are transported through the drum because of the flow drag and the rotational motion of cylinder which is defined as 5 1/s. The gas phase medium is specified as hot air that is in direct contact with the particles. Three different sizes of particles are considered as diameter of 20 mm, half size 10 mm and fifth size 4 mm. In order to evaluate the effects of particle size distribution, three main cases (Case1-3 in Table 1) are defined so that the mass of the bed remains *constant* at 156.6 g. At the first case, all particles have the same diameter of 20 mm (Figure 3.b). For the second and third cases, the procedure is keeping half the mass (78.3 g) with diameter of 20 mm, and the other half of mass with diameter of 10 mm and 4 mm, respectively (Figure 3.c, 3.d), although the total bed mass stays still *constant*. As can be seen in the Table 1 with decreasing the particle size, the number of particles and thus the surface area of the bed increases so that it influences the heat transfer between the solid and gas phases which is discussed later. The Figure 3 shows the drum case geometry including a packed bed of particles with different sizes as distributed randomly. As can be seen, the hot air enters to the drum and encounters with particles while drum is rotating that helps to speed up drying and the cool air exits the drum after exchanging heat with particles.

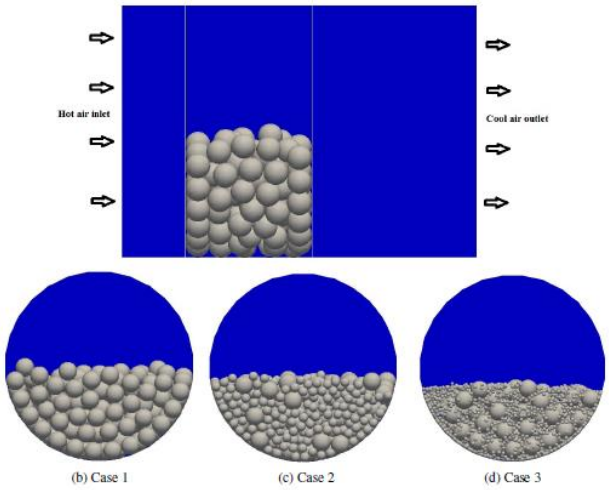

Figure 3 The schematic of the rotary dryer including different particle size distribution

Table 1 Particle size distribution for different cases

Case	*d_p [mm]*	*Particle No.*	*Bed mass[g]*	*SA [m^2]*	*SA_{total} [m^2]*	*SA change*
1	20	25	78.3	0.03416	0.06832	--
	20	25	78.3	0.03416		
2	20	25	78.3	0.03416	0.09699	+42%
	10	200	78.3	0.06283		
3	20	25	78.3	0.03416	0.22540	+230%
	4	3125	78.3	0.15708		
4	10	200	78.3	0.06283	0.21991	+222%
	4	3125	78.3	0.15708		
5	10	200	78.3	0.06283	0.12566	+84%
	10	200	78.3	0.06283		
6	4	3125	78.3	0.15708	0.31416	+360%
	4	3125	78.3	0.15708		

Effect of surface area on drying rate

The Figure 4 demonstrates drying rate behaviour at the gas temperature of 350 °C and pressure of 1 bar. It should be noted that during drying process in the rotary dryers, there is no constant-rate period which means that drying happens only in the falling-rate period [13]. This is shown in Figure 4 so that after reaching to the highest rate, instead of staying at constant rate similar to part *AB* for single particle (Figure 4), it falls down till finishing the moisture content. On the other hand, in addition to an increase in the gas flow rate which causes an increase in heat transfer rate between gas-particles and the drying rate augments [7], changing particle size distribution to raise surface area also boosts the drying rate. According to the Table 1 which represents increasing surface area with regards to different combination of particle size distribution, it could be seen that with increasing the surface area from Case 1 to Case 6, the critical moisture content is higher as well as reducing drying time. In other words, comparing the Case 1 (the base case with homogeneous particle size of 20 mm) and the Case 6 (distribution of size 4 mm), with increasing the surface area to 360 % (Table 1) the drying rate is enhanced from 0.00024 kg water/s to 0.00052 kg water/s so that the growth is considerably more than twice. From time point of view, at Case 1 all particles are dried completely after 2 s while at Case 6 the drying time is shortened to 0.6 s which displays effect of surface area increment to reduce residence time.

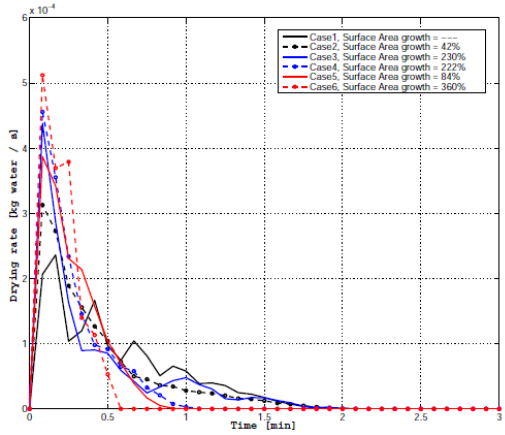

Figure 4 Drying rate vs. time

Effect of surface area on heat loss

This section significantly depicts the influence of surface area growth on heat loss quantity. In Figure 5 three cases (Case 1-3) are considered so that increasing surface area leads to rising the bed mean total energy earlier and faster drying. The lines show the cases with adiabatic wall in contrary to dash-lines showing non-adiabatic wall with initial ambient temperature. As expected, all cases start from the same point and they finish at the same point when there is no heat exchange between particles and drum wall (adiabatic). In order to investigate the effect of surface area, the dash-lines represent the cases when the drum wall is non-adiabatic. That is, there exist conductive and radiative heat transfer between the particles and drum wall which leads to lose heat. Thus, it is obvious that the blue dash-line (Case 3) is the highest and the black dash-line (Case 2) is higher than the red dash-line (Case 1). This means that with increasing surface area, the heat loss is reduced which makes the drying more efficient. The reason is the surface area growth improves the rate of convective heat transfer between the gas and particulates which clarifies with better heat transfer rate, the lost energy is diminished accordingly.

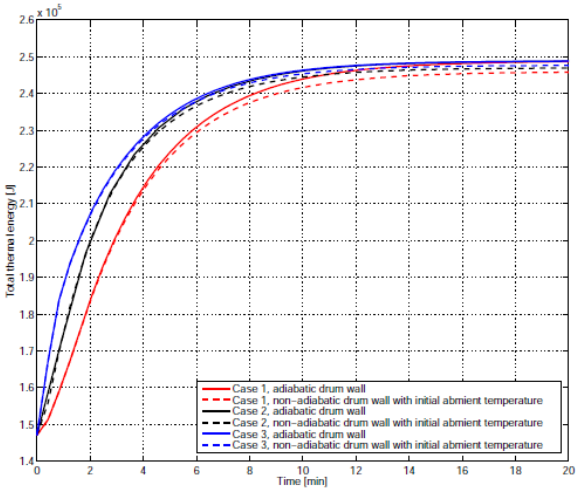

Figure 5 Total thermal energy vs. time

Inlet gas velocity

Figure 6.a and 6.b compare prediction of particle bed mean temperature and moisture content based on the different inlet gas velocity (1, 1.5, 2 m/s) for Case 1-2. As stated, higher inlet gas velocity leads to better heat transfer rate and enhanced drag force acting on the particles which causes more dispersed bed, leading to less drying time. This is expressed according to dominant convective heat transfer rather than conductive heat transfer inside particle which is not effected by gas flow rate. It could be seen from Figure 6.a that the bed mean temperature starts at initial temperature of 95 °C (heat-up is not considered) and finishes to the gas temperature 350 °C expectedly. Increasing inlet gas velocity leads to rise the bed mean temperature sooner and thus drying is faster. Similarly, the behaviour of the bed moisture content is shown in Figure 6.b which is started from initial value defined as 5 db% and total

drying occur when all water are evaporated and it reaches to zero. Then the added heat is used to raise particle temperature until gas temperature. Obviously, with increasing gas velocity the bed moisture content drops sooner and consequently drying is quicker.

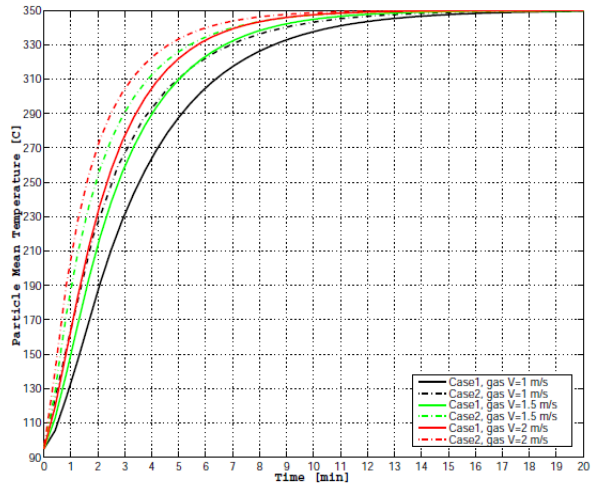

(a) Bed mean temperature with different inlet gas velocity for Case1-2 vs. time

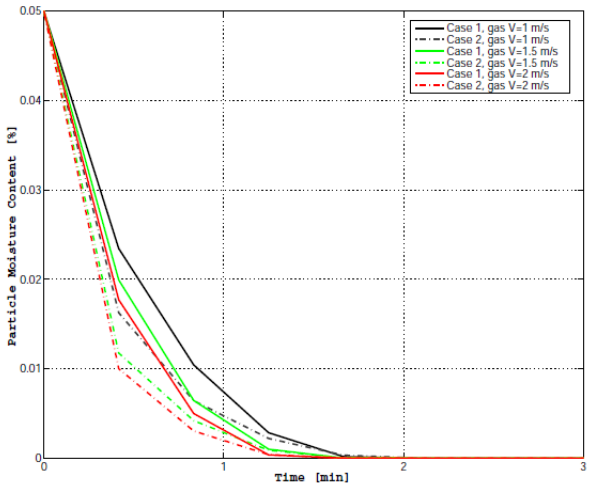

(b) Bed mean temperature with different inlet gas velocity for Case1-2 vs. time

Figure 6 Effect of inlet gas velocity on bed mean temperature and moisture content

Inlet gas temperature

The influence of gas temperature on the particle bed mean temperature and bed moisture content are shown in Figure 7.a and 7.b for Case 1-2. The strict and dash lines show different gas temperatures for Case 1 and 2, respectively. The dash lines show that at the same temperature with 42 % higher contact surface area of Case 2 rather than Case 1, the drying is faster as discussed previously. In addition, with increasing inlet gas temperature (210, 280 and 350 °C), it could be seen that the particle mean temperature rises earlier and moisture content of the bed evaporates sooner. This is explained as with higher gas temperature, the conductive heat transfer also increases. In another words, because of higher gas temperature there is more heat and driving force acting on the particles which consequently leads to faster drying.

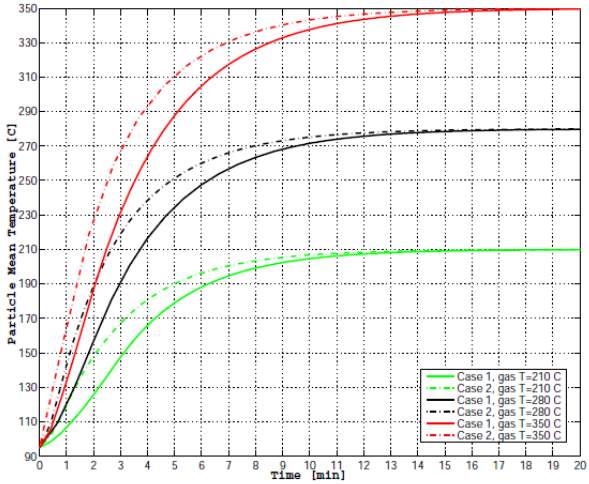

(a) Bed mean temperature with different inlet gas temperature for Case1-2 vs. time

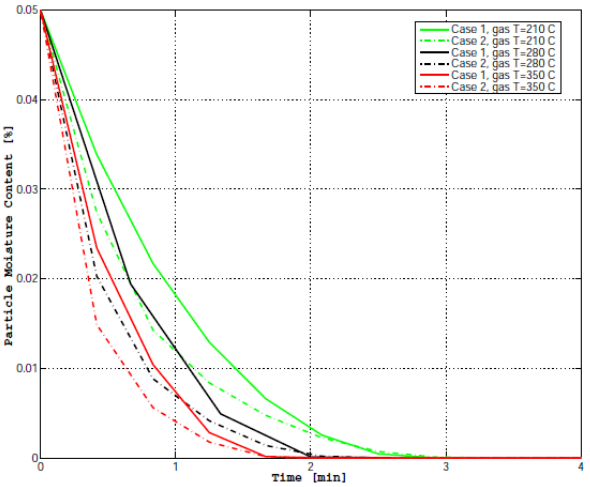

(b) Bed mean moisture content with different inlet gas temperature for Case1-2 vs. time

Figure 7 Effect of inlet gas temperature on bed mean temperature and moisture content

Temperature distribution of particles

The temperature distribution of particles is visually presented in Figure 8-9 at four different instances (10, 60, 150, 240 s) in order to investigate the influence of particle size distribution. After 10 s, the particles in Case 1 are homogeneously close to saturation temperature (below 100 °C) but drying is not started yet. While in Case 2 the small particles at first layer close to the gas inlet are started to dry, even although the big particles and small ones behind the first layer need still more energy to reach to the saturation temperature. In Case 3 the smallest particles at first layer are already dried and rear ones are started to dry but big particles still require more time to start drying. By injecting hot gas continuously, at 60 s

the surface temperature of particles in Case 1 passed the saturation temperature which shows the surface is dried and the drying front is traversed from the surface towards the particle core. While in Case 2 the surface temperature of smaller particles are higher than big ones owing to the lower surface area. And that is why in Case 3, the surface temperature of smallest particles at first layer are quite near gas temperature. As a result, with passing the time to 150 s and 240 s according to the Figure 9 (left and right), comparison of surface temperature show that whatsoever the particle size is smaller, the drying heat required is lower which leads to faster drying and reaching to the gas temperature sooner.

CONCLUSION

In this study, drying process of wet spherical woods in a rotary drum is investigated considering particles dynamics motion with employing eXtended Discrete Element Method. To prove this approach, the drying is validated with experiment for a single particle via temperature and moisture content behaviour so that the results show a good agreement. The case study is a drum rotating with a constant angular velocity involving moist particles as a packed bed at the beginning of process. The focus of this work is verifying the effect of particle size distribution on drying rate and heat loss. In case of drying rate, there is no constant-rate period and it takes place in falling-rate period only. In addition, it is indicated that with smaller particles in the system, the critical drying rate is higher as well as heat loss to the wall because of conduction and radiation heat transfer between particles and wall is lower whereby the system is more efficient. The reason is mentioned as with decreasing the particle size while keeping mass of the bed constant, the surface area is increased which leads to higher convective heat transfer rate between particles and gas phase and eventuates to faster drying. Moreover, the bed mean temperature and water content graphs demonstrate that with increasing gas inlet temperature and velocity, the drying time is less as anticipated. Finally, the temperature distribution of particles are shown visually at four different instances during drying which represent bigger particles take longer time to move drying front from surface to core and reach to the gas phase temperature at a later time.

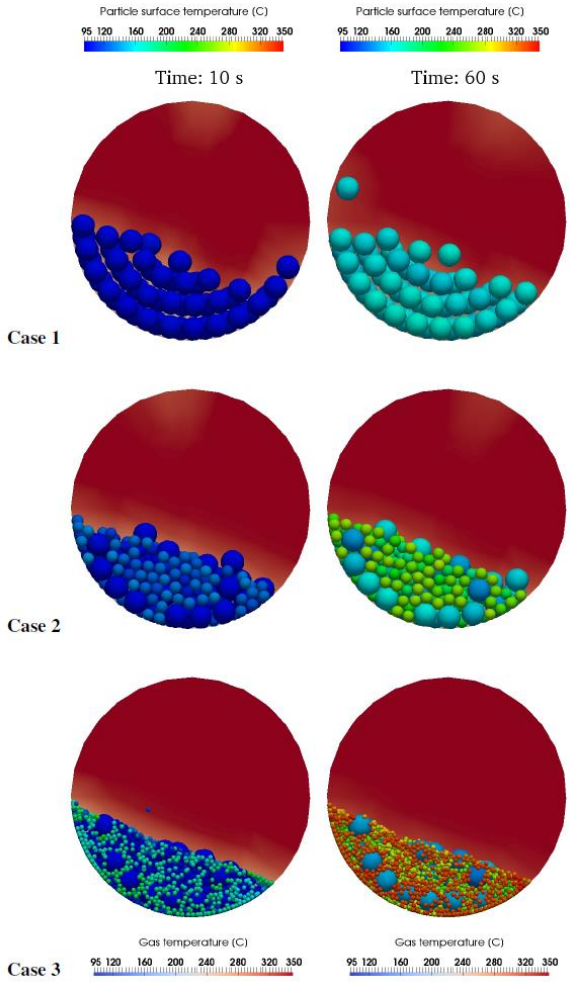

Figure 8 Temperature distribution of particles for Case1-3, left: at 10[s], right: at 60[s]

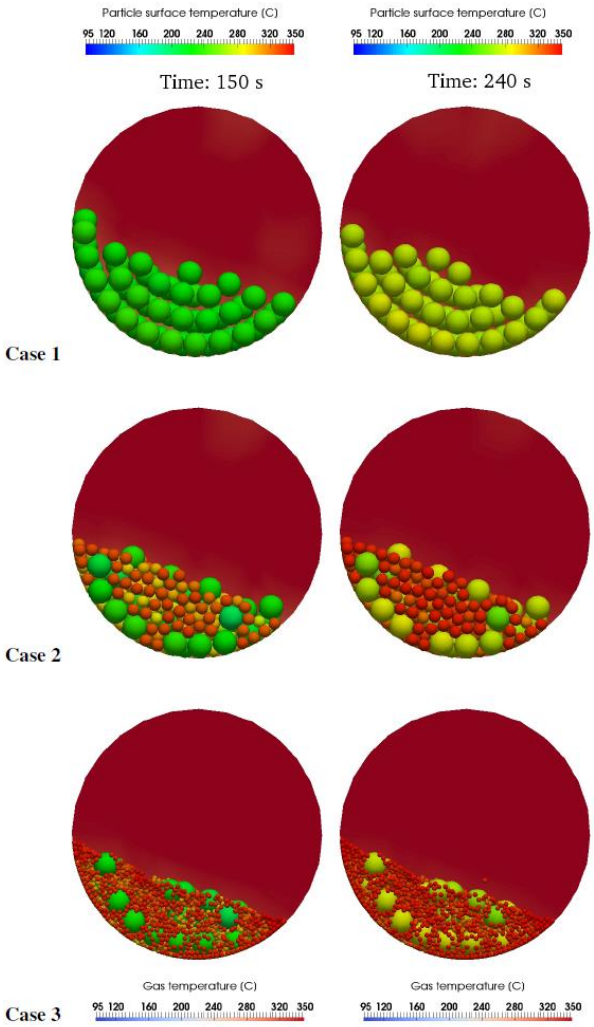

Figure 9 Temperature distribution of particles for Case1-3, left: at 150[s], right: at 240[s]

REFERENCES

[1] Perazzini, H., Freire, F. B., Freire, J. T., Prediction of residence time distribution of solid wastes in a rotary dryer, *Drying Technology*, Vol. 32, 2014, pp. 428–436

[2] McCabe, W., Smith, J., Harriott, P., *Unit Operations of Chemical Engineering 4th Ed*, McGraw-Hill, New York, 1987

[3] Ademiluyi, F. T., Abowei, M. F. N., Puyate, Y. T., Achinewhu, S. C., Effects of drying parameters on heat transfer during drying of fermented ground cassava in a rotary dryer, *Drying Technology*, Vol. 28, 2010, pp. 550–561

[4] Mujumdar, A. S., *Handbook of Industrial Drying 4th Ed*, CRS Press, 2006

[5] Stroem, L., Desai, D., Hoadley, A., Superheated steam drying of brewers spent grain in a rotary drum, *Advanced Powder Technology*, *Vol.* 20, 2009, pp. 240–244

[6] Xu, Q., Pang, S., Mathematical modelling of rotary drying of woody biomass, *Drying Technology*, Vol. 26, 2008, pp. 1344–1350

[7] Abbasfard, H., Rafsanjani, H. H., Ghader, S., Ghanbari, M., Mathematical modeling and simulation of an industrial rotary dryer: A case study of ammonium nitrate plant, *Powder Technology*, Vol. 239, 2013, pp. 499–505

[8] Fernandes, N. J., Atade, C. H., Barrozo, M. A. S., Modelling and experimental study of hydrodynamic and drying characteristics of an industrial rotary dryer, *Brazilian Journal of Chemical Engineering*, Vol. 26, 2009, pp. 331–341

[9] Renaud, M., Thibault, J., Alvarez, P. I., Influence of solids moisture content on the average residence time in a rotary dryer, *Drying Technology*, Vol. 19, No.9, 2001, pp. 2131–2150

[10] Ademiluyi, F. T., Abowei, M. F. N., Theoretical model for predicting moisture ratio during drying of spherical particles in a rotary dryer, *Modelling and Simulation in Engineering*, Vol. 2013, 2013, 7 pages

[11] Johnson, P., Paliwal, J., Cenkowski, S., Analysing the effect of particle size on the disintegration of distiller's spent grain compacts while drying in superheated steam medium, *Biosystems Engineerin*, Vol. 134, 2015, pp. 105–116

[12] Castano, F., Rubio, F. R., Ortega, M. G., Modeling of a cocurrent rotary dryer, *Drying Technology*, Vol 30, 2012, pp. 839–849

[13] Iguaz, A., Esnoz, A., Martinez, G., Lopez, A., Virseda, P., Mathematical modelling and simulation for the drying process of vegetable wholesale by-products in a rotary dryer, *Journal of Food Engineering*, Vol. 59, 2003, pp. 151–160

[14] Perry, R. H., Perry's Chemical Engineers Handbook, McGraw-Hill, 1997

[15] Mahmoudi, A. H., Hoffmann, F., Peters, B., Application of xdem as a novel approach to predict drying of a packed bed, *International Journal of Thermal Sciences*, Vol. 75, 2014, pp. 65–75

[16] Faghri, A., Zhang, Y., Transport Phenomena in Multiphase Systems, Elsevier Academic Press, 2010

[17] Peters, B., The extended discrete element method (xdem) for multi-physics applications, *Scholarly Journal of Engineering Research*, Vol. 2, 2013, pp. 1–20

[18] Hager, J., Hermansson, M., Wimmerstedt, R., Modelling steam drying of a single porous ceramic sphere experiments and simulations, *Chemical Engineering Science*, Vol. 52, 1997, pp. 1253–1264

[19] Bellais, M., Modelling of the pyrolysis of large wood particles, Ph.D. thesis, Royal Institute of Technology (KTH), 2007

[20] Gronli, M., A theoretical and experimental study of the thermal degradation of biomass, Ph.D. thesis, The Norwegian University of Science and Technology, 1996

[21] Peters, B., DÅiugys, A., Navakas, R., Simulation of thermal conversion of solid fuel by the discrete particle method, *Lithuanian Journal of Physics*, Vol. 51, 2011, pp. 91–105

[22] Peters, B., Classification of combustion regimes in a packed bed based on the relevant time and length scales, *Combustion and Flame*, Vol. 116, 1999, pp. 297–301

[23] Peters, B., Numerical simulation of heterogeneous particle combustion accounting for morphological changes, *27th International Conference on Environmental Systems*, Lake Tahoe, USA, SAE-paper 972562, July 1997

[24] Looi, A., Golonka, K., Rhodes, M., Drying kinetics of single porous particles in superheated steam under pressure, *Chemical Engineering Journal*, Vol. 87, 2002, pp. 329–338